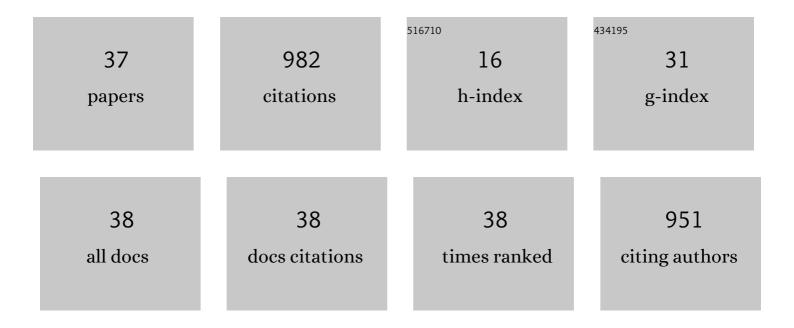
## **Xuzhong Gong**

List of Publications by Year in descending order

Source: https://exaly.com/author-pdf/4616523/publications.pdf Version: 2024-02-01



#	Article	IF	CITATIONS
1	Selfâ€&upporting Porous CoPâ€Based Films with Phaseâ€&eparation Structure for Ultrastable Overall Water Electrolysis at Large Current Density. Advanced Energy Materials, 2018, 8, 1802445.	19.5	114
2	Reactivity of pulverized coals during combustion catalyzed by CeO2 and Fe2O3. Combustion and Flame, 2010, 157, 351-356.	5.2	111
3	Hierarchically 3D porous films electrochemically constructed on gas–liquid–solid three-phase interface for energy application. Journal of Materials Chemistry A, 2017, 5, 9488-9513.	10.3	76
4	Variation on anthracite combustion efficiency with CeO2 and Fe2O3 addition by Differential Thermal Analysis (DTA). Energy, 2010, 35, 506-511.	8.8	74
5	ORR and OER of Co–N codoped carbon-based electrocatalysts enhanced by boundary layer oxygen molecules transfer. Carbon, 2021, 172, 556-568.	10.3	65
6	Comparative Study of CeO <sub>2</sub> and Doped CeO <sub>2</sub> with Tailored Oxygen Vacancies for CO Oxidation. ChemPhysChem, 2011, 12, 2763-2770.	2.1	56
7	Impurities Removal from Metallurgical-Grade Silicon by Combined Sn-Si and Al-Si Refining Processes. Metallurgical and Materials Transactions B: Process Metallurgy and Materials Processing Science, 2013, 44, 828-836.	2.1	53
8	Millisecond Conversion of Photovoltaic Silicon Waste to Binderâ€Free High Silicon Content Nanowires Electrodes. Advanced Energy Materials, 2021, 11, 2102103.	19.5	48
9	Relation between Sticking and Metallic Iron Precipitation on the Surface of Fe2O3 Particles Reduced by CO in the Fluidized Bed. ISIJ International, 2011, 51, 1403-1409.	1.4	42
10	N-Doped gel-structures for construction of long cycling Si anodes at high current densities for high performance lithium-ion batteries. Journal of Materials Chemistry A, 2019, 7, 11347-11354.	10.3	29
11	Insight of Iron Whisker Sticking Mechanism from Iron Atom Diffusion and Calculation of Solid Bridge Radius. Metallurgical and Materials Transactions B: Process Metallurgy and Materials Processing Science, 2014, 45, 2050-2056.	2.1	25
12	Preparation of CaO-containing carbon pellet from recycling of carbide slag: Effects of temperature and H3PO4. Waste Management, 2019, 84, 64-73.	7.4	22
13	Characterization of Precipitated Carbon by XPS and Its Prevention Mechanism of Sticking during Reduction of Fe2O3 Particles in the Fluidized Bed. ISIJ International, 2013, 53, 411-418.	1.4	20
14	Progress toward Electrochemistry Intensified by using Supergravity Fields. ChemElectroChem, 2015, 2, 1879-1887.	3.4	20
15	Time-Dependent Surface Structure Evolution of NiMo Films Electrodeposited Under Super Gravity Field as Electrocatalyst for Hydrogen Evolution Reaction. Journal of Physical Chemistry C, 2017, 121, 16792-16802.	3.1	20
16	Sulfur removal from bauxite water slurry (BWS) electrolysis intensified by ultrasonic. Ultrasonics Sonochemistry, 2015, 26, 142-148.	8.2	19
17	Alumina Hydrate Polymorphism Control in Al–Water Reaction Crystallization by Seeding to Change the Metastable Zone Width. Crystal Growth and Design, 2016, 16, 1056-1062.	3.0	16
18	Mechanism Analysis of Carbon Contamination and the Inhibition by an Anode Structure during Soluble K <sub>2</sub> CrO <sub>4</sub> Electrolysis in CaCl <sub>2</sub> -KCl Molten Salt. Journal of the Electrochemical Society, 2017, 164, E360-E366.	2.9	16

**XUZHONG GONG** 

#	Article	IF	CITATIONS
19	Inâ€situ synthesis of NaP zeolite doped with transition metals using fly ash. Journal of the American Ceramic Society, 2019, 102, 7665-7677.	3.8	16
20	Competition of Oxygen Evolution and Desulfurization for Bauxite Electrolysis. Industrial & Engineering Chemistry Research, 2017, 56, 6136-6144.	3.7	15
21	Roles of Electrolyte Characterization on Bauxite Electrolysis Desulfurization with Regeneration and Recycling. Metallurgical and Materials Transactions B: Process Metallurgy and Materials Processing Science, 2017, 48, 726-732.	2.1	14
22	The Importance of Slag Structure to Boron Removal from Silicon during the Refining Process: Insights from Raman and Nuclear Magnetic Resonance Spectroscopy Study. Metallurgical and Materials Transactions B: Process Metallurgy and Materials Processing Science, 2017, 48, 3239-3250.	2.1	12
23	Constructing an artificial boundary to regulate solid electrolyte interface formation and synergistically enhance stability of nano-Si anodes. Journal of Colloid and Interface Science, 2022, 619, 158-167.	9.4	12
24	Desulfurization from Bauxite Water Slurry (BWS) Electrolysis. Metallurgical and Materials Transactions B: Process Metallurgy and Materials Processing Science, 2016, 47, 649-656.	2.1	10
25	Electrochemical preparation of V2O3 from NaVO3 and its reduction mechanism. Journal Wuhan University of Technology, Materials Science Edition, 2017, 32, 1019-1024.	1.0	10
26	Roles of Ultrasound on Hydroxyl Radical Generation and Bauxite Desulfurization from Water Electrolysis. Journal of the Electrochemical Society, 2018, 165, E177-E183.	2.9	10
27	A flexible and conductive connection introduced by cross-linked CNTs between submicron Si@C particles for better performance LIB anode. Nanoscale Advances, 2021, 3, 2287-2294.	4.6	10
28	Relationship Between Iron Whisker Growth and Doping Amount of Oxide During Fe2O3 Reduction. Metallurgical and Materials Transactions B: Process Metallurgy and Materials Processing Science, 2016, 47, 1137-1146.	2.1	8
29	Catalytic Effects of CeO <sub>2</sub> /Fe <sub>2</sub> O <sub>3</sub> and Inherent Mineral Matter on Anthracite Combustion Reactions and Its Kinetic Analysis. Energy & Fuels, 2017, 31, 12867-12874.	5.1	8
30	Design of Refining Slag Based on Raman and NMR Spectroscopy Study for Removing Phosphorus for SoG-Si. Silicon, 2020, 12, 171-183.	3.3	8
31	Oxygen Reduction Reaction from Water Electrolysis Intensified by Pressure and O <sub>2</sub> <sup>â^`</sup> Oxidation Desulfurization. Journal of the Electrochemical Society, 2018, 165, E139-E147.	2.9	7
32	Fe <sub>3</sub> C doped modified nano-Si/C composites as high-coulombic-efficiency anodes for lithium-ion batteries. Sustainable Energy and Fuels, 2021, 5, 6170-6180.	4.9	5
33	Short-Process Multiscale Core–Shell Structure Buffer Control of a Ni/N Codoped Si@C Composite Using Waste Silicon Powder for Lithium-Ion Batteries. ACS Applied Energy Materials, 2022, 5, 178-185.	5.1	5
34	Boehmite Preparation via Alditols-Interacting Transformation of Metastable Intermediates in Al–H <sub>2</sub> O Reaction Crystallization. Crystal Growth and Design, 2017, 17, 183-190.	3.0	4
35	Study on hydrocyclone separation enhancement of micro Si/SiC from silicon-sawing waste by selective comminution. Separation Science and Technology, 2021, 56, 991-999.	2.5	2
36	Millisecond Conversion of Photovoltaic Silicon Waste to Binderâ€Free High Silicon Content Nanowires Electrodes (Adv. Energy Mater. 40/2021). Advanced Energy Materials, 2021, 11, .	19.5	0

#	Article	IF	CITATIONS
37	Rationally designed highâ€conductivity <i>Hydrangea macrophylla</i> â€like Si@NiO@Ni/C composites as a highâ€performance anode material for lithiumâ€ion batteries. Electrochemical Science Advances, 0, , .	2.8	ο